DETERMINING SIZE AND LOCATION OF SUBSURFACE DEFECT OF STEEL PLATE BY LOCK-IN THERMOGRAPHY

Kisoo Kang[1], Manyong Choi[1], Jeonghak Park[1], Wontae Kim[2], Koungsuk Kim[3], Seongmo Yang[4]

[1]Korea Research Institute of Standard and Science, Daejeon, 305-600 South Korea
[2]Kongju National University, Chungnam, 340-702 South Korea
[3]Chosun University, Gwangju, 501-759 South Korea
[4]Chonbuk National University, Jeonju, 561-756 South Korea

Abstract

The paper describes the quantitative determination of the size and the location of a subsurface defect from the phase image of lock-in infrared thermography. Phase (or temperature) difference between a defect area and a sound area indicates the qualitative location and size of a defect. To accurately estimate those, the paper proposes a shearing phase technique in which the inspected image is shifted with a proper pixel size to obtain the shearing image and the subtraction between two images gives a shearing phase distribution. The shearing phase distribution has the maximum, the minimum, and zero point which is a key to quantitatively determine the size and the location of subsurface defect. Experimental results of steel plate with artificial defects show good agreement with actual values.

1. Introduction

Infrared thermography (IRT) provides colorful images of concerning area where local changes of surface temperature indicate subsurface defects. Over the years, IRT is intensively being used by nondestructive evaluation engineers for damage detection in materials[1,2]. Since most of these applications in nondestructive testing (NDT) rely on the temperature differences between defect and sound part, artifacts (local non-uniform emissivity on surface, air turbulences, reflections from the environment and etc) might give rise to a misconception. Also, Materials of high thermal conductivity (diffusivity) are subjected to too rapid propagation which is with consequent weak image contrast. Detecting sensitivity of IRT is progressively improved by lock-in technique[3-5]. The basic idea of lock-in infrared thermograpphy (Lock-in IRT) is that the temperature modulation induced from the outside on the surface of the inspected component propagates as harmonic thermal wave. As this wave undergoes reflections at boundaries like all other waves, the phase at the surface is modified by the thermal waves coming back from the inside of the material. The modified thermal waves transmit the inside information to infrared camera and the resulting change of the thermal image is analyzed to separate real signal from accidental signals. Lock-in IRT allows for deeper defect inspection than conventional IRT and is less sensitive to environmental disturbances.

In the 1970's, the stress intensity factor in fracture mechanics revealed the need for quantitative nondestructive evaluation (QNDE) of a defect by NDT. In QNDE, defects are evaluated based on their characteristics such as position, size, shape and kind. Based on this factor, the reliability and life of a structure can be evaluated[6]. IRT had to include QNDE without exception. To meet such a demand, researchers had to study quantitative determination by theoretical analysis and practical applications[7-9]. This paper proposes a simple and practical technique for the quantitative determination of the size and the location of a subsurface defect. In technique, original image is shifted with a pixel size to create a shearing image and the subtraction between two images gives a shearing phase or temperature distribution, which has the maximum, the minimum, and zero point. These positions are a key to quantitatively determine the size and the location of a defect.

2. Lock-in thermography

The basic concepts of lock-in IRT were first described by Carlomagno and Berardi [10]. Basically, in lock-in analysis the heat source induced from outside has to be calibrated (for each excited frequency) to endure that the temperature waveform of heat source is really sinusoidal and IR camera collects a series of thermal images and compares their temperature extracting sinusoidal wave pattern at each pixel of the images , as shown in Fig. 1. The sinusoidal temperature $T(x, y)$ at the surface($z = 0$) in one dimension is given by

$$T(x, y) = Ae^{i[wt - f(x,y)]} \quad (1)$$

where, A is the thermal wave amplitude and $f(x,y)$ is the phase on image plane. The surface temperature field can be reconstructed by only the collected 3 or 4 thermal images with the phase step of $T/4$.

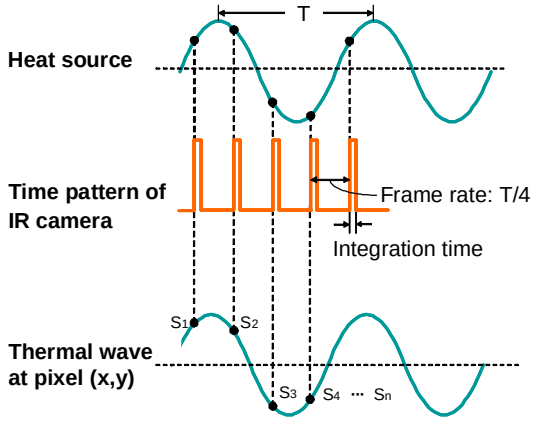

Figure 1: *Principle of lock-in thermography*

These four images S_n are used to derive the magnitude image $A(x,y)$ and phase image $f(x,y)$. The calculation is quit simple to obtain amplitude and phase of temperature field as given by[4]:

$$f(x,y) = \tan^{-1}\left(\frac{S_1(x,y) - S_3(x,y)}{S_2(x,y) - S_4(x,y)}\right) \quad (2)$$

$$A(x,y) = \sqrt{(S_1(x,y) - S_3(x,y))^2 + (S_2(x,y) - S_4(x,y))^2} \quad (3)$$

As compared with those in conventional thermal images, the phase image is more useful for quantitative evaluation of metal material because contrast changes at the defects can be more clearly observed. The defect in lock-in IRT is defined as phase difference, which is the difference between the phase of defect area and that of sound area[11]. The phase difference, $\Delta f(x,y)$ on each pixel of thermal image between a defect area and a sound area is defined as equation (4).

$$\Delta f(x,y) = f_d(x,y) - f_s(x,y) \quad (4)$$

where $f_d(x,y)$ is the phase of a pixel (x,y) on a defect area, and $f_s(x,y)$ is the phase of a pixel (x,y) on a sound area. The phase differences at an object surface have sufficient information about the shape and the location of a subsurface defect and the boundary of a defect results in the maximum and minimum phase change which is a key in determining the size and the location of a defect. The slope in this paper can be easily extracted by a shearing phase technique, in which shearing phase, f_{SP} is obtained by the subtraction between adjacent phases with equation (5).

$$\Delta f_{SP} = \Delta f(x+1,y) - \Delta f(x,y) = f(x+1,y) - f(x,y) \quad (5)$$

The equation means the subtraction between a original image and the image shifted with a proper pixel in x-direction or y-direction. The shearing phase distribution provides the maximum, the minimum, and zero phases.

3. Specimen and experimental procedure

Stainless steel plates (AISI304) with different depth, shape, and size are prepared as shown Fig. 2. Specimen I with 4 flat-bottom-holes at different depths is modeled on wall thinning of piping system. Specimen II and III with penetrated rectangular holes at different size and depth are modeled on a subsurface void. The lock-in IRT system used in the work is silver 480, Cedip, France. It consists of an infrared camera with lock-in module, system controller, function generator, and a heat sources (1 kW halogen lamp) as shown Fig. 3.

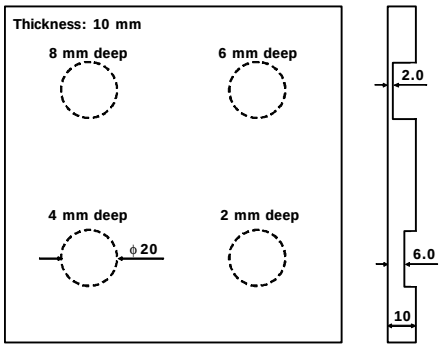

(a) Specimen I

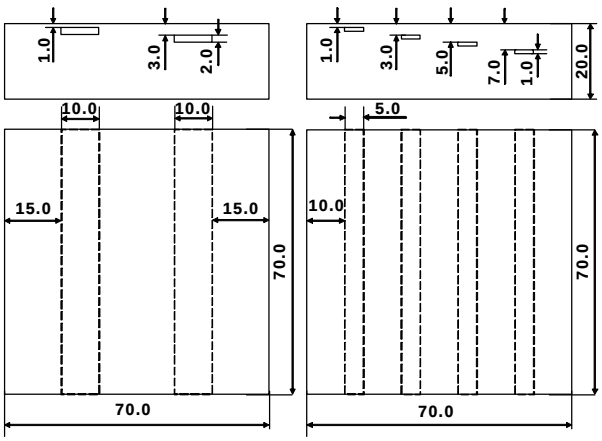

(b) Specimen II (c) Specimen III

Figure 2: *Stainless steel specimen*

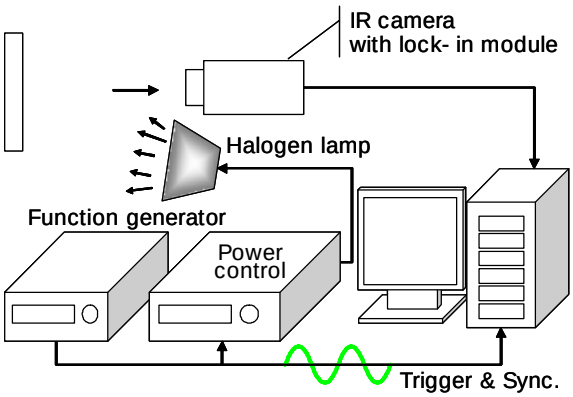

Figure 3: *Lock-in Thermography system*

The heat source is driven by power controller; the source and camera are synchronized with sinusoidal function of function generator. The phase images are automatically calculated with Eq. (2) in each heat generating frequency. In experiment, the blind frequency[11] in which the returning wave is in phase with the incident wave is avoided by obtaining the phase difference at each thermal wave frequency and the optimum frequency giving maximum phase difference is selected for apply the shearing phase technique.

4. Results

4.1. Specimen I: back drilled circular hole

Figure 4 shows the defects of specimen I detectable using phase image. The 6 and 8 *mm* deep defects are clearly recognized, however the 4 and 2 *mm* deep defects are difficult to be detected with a halogen lamp (1kW). The phase differences between the central point values of the each detect and the average phase values of the sound area are plotted in Fig. 5. From Fig. 5, it can be observed that the blind frequency of 8 *mm* deep defect exists nearby 40 mHz and 10 mHz is selected for maximum phase difference. Figure 6(a) shows the phase difference induced with 10 mHz on the central point of defect with 6 and 8 *mm* deep. Although the location can be defined as the maximum phase differences, it is difficult to directly determine defect sizes.

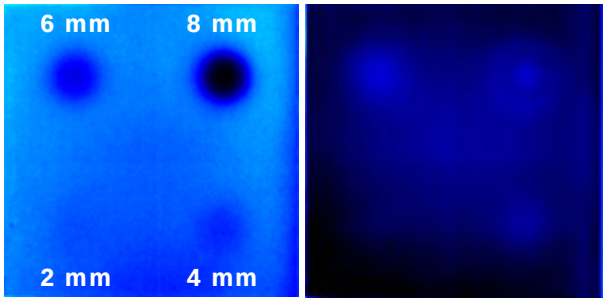

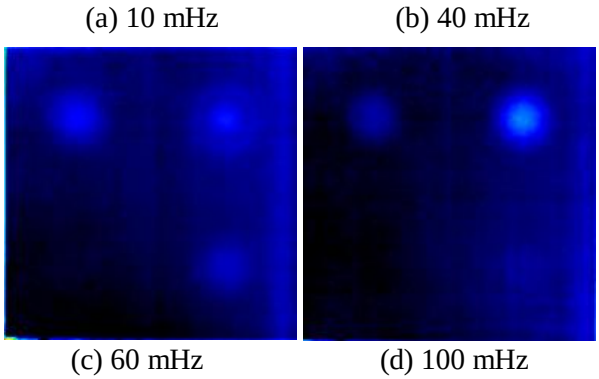

Figure 4: *Phase image of specimen I*

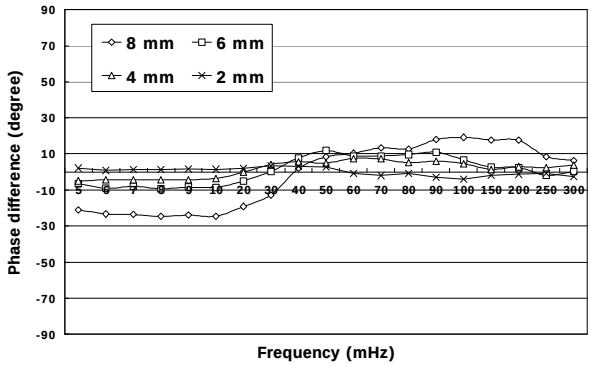

Figure 5: *Phase differences at each defect of specimen I*

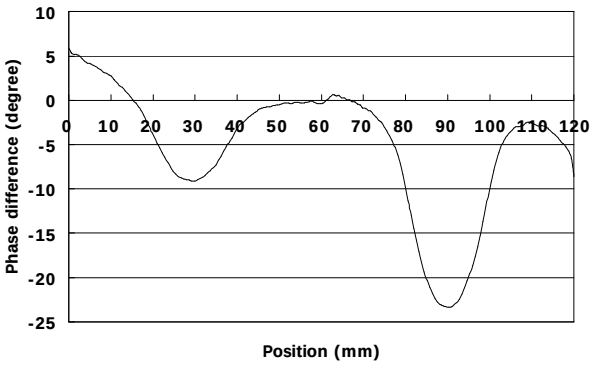

(a) Phase difference on 6 and 8 *mm* deep defects

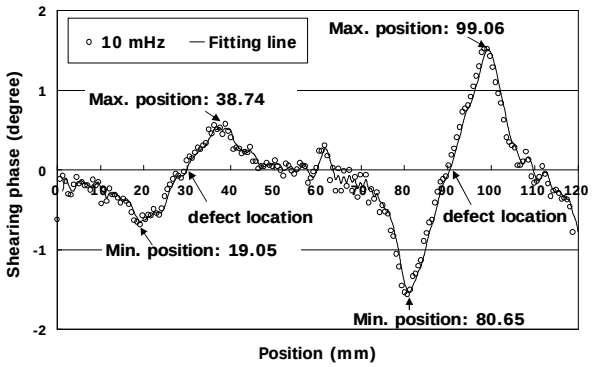

(b) Shearing phase

Figure 6: *Quantitative determination of the size and the location of defects*

The shearing phase profile from the subtraction between pixels is shown as Fig. 6(b). The size and the location of defects can be quantitatively determined with the phase image of Fig. 4(a) and the shearing phase of Fig. 6(b). In Fig. 6(b), the distance between the maximum and the minimum shearing phase is estimated as the size of the defect and the zero point of shearing phase is defined as the location. The size of 6 *mm* deep defect is evaluated as 19.69 *mm* and the size of 8 mm deep defect is as 18. 41 *mm*, which is agreed with actual defect size well. With the zero point of shearing phase, the central location of 6 *mm* deep defect is positioned at 30 *mm* from the left of specimen and 8 *mm* deep defect is at 90 *mm* respectively, which also shows good agreement with actual location well.

4.2. Specimen II: penetrated rectangular holes (10 *mm* width and 2 *mm* height)

Rectangular holes of 10×2 mm^2 pass through 20 *mm* thick steel plate, which are at 1 *mm* and 3 *mm* depth respectively. Figure 7 shows the inspection results in which two defects are clearly distinguished. The size and the location of these detects are evaluated with Fig. 8. Figure 8(a) plots the phase difference, of which the shearing phase profile is shown as Fig. 8(b). Two frequencies give the same trend in shearing phase and the profile of 30 mHz is selected for the determination.

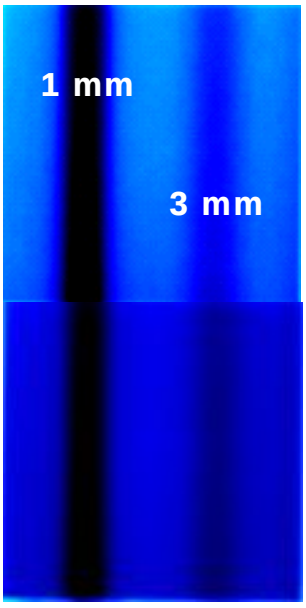

(a) 30 mHz (b) 10 mHz

Figure 7: *Phase image of specimen II*

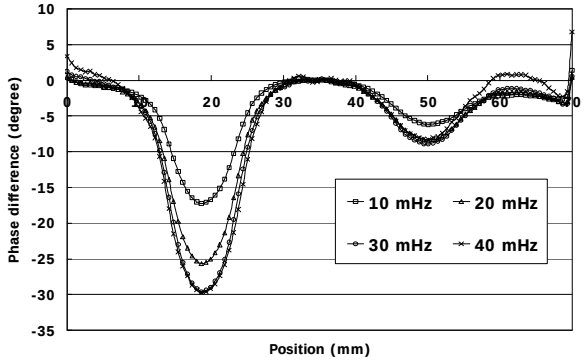

(a) Phase differences according to each heat generation frequencies

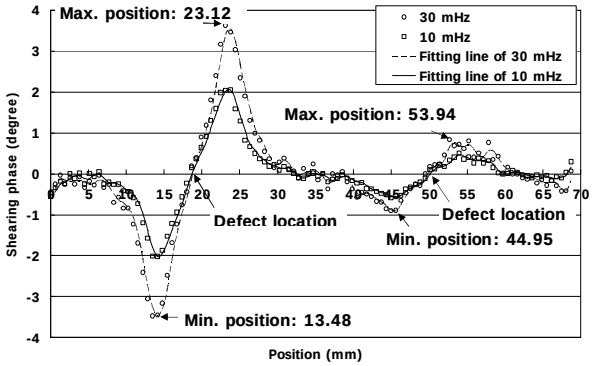

(b) Shearing phase

Figure 8: *Quantitative determination of the size and the location of defects in specimen II*

Compared with Fig. 7, the maximum, minimum, and zero point of shearing phase are defined and the size of defect is estimated as 9.64 *mm* and 8.99 *mm* respectively. The location of defects is 19 *mm* and 50 *mm* respectively. The inspection results at each frequency are agreed with actual values of specimen II.

4.3. Specimen III: penetrated rectangular holes (5 *mm* width and 1 *mm* height)

In Fig. 9, the penetrated rectangular holes at 1 and 3 *mm* depth are detectable at thermal wave frequency of 40 mHz. Phase difference profile at the middle of specimen is plotted to Fig. 10(a) and the size and the location of defects are estimated with Fig. 10(b).

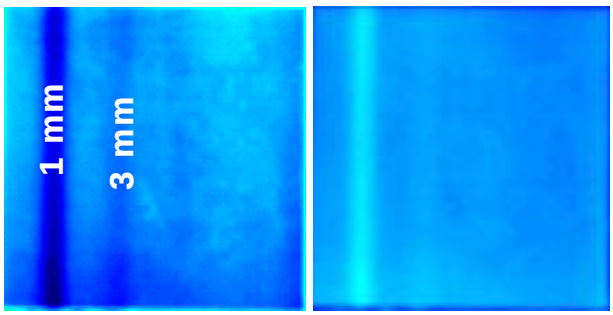

(a) 40 mHz (b) 60 mHz

Figure 9: *Phase image of specimen III*

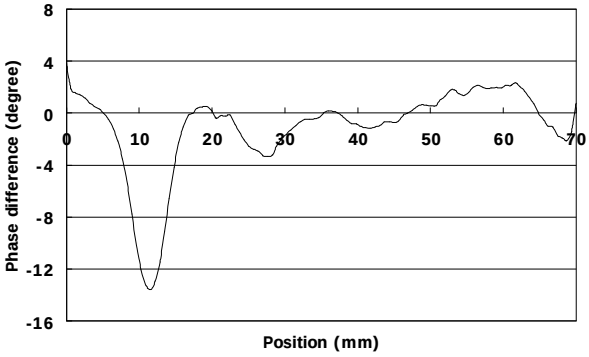

(a) Phase difference at the middle of specimen

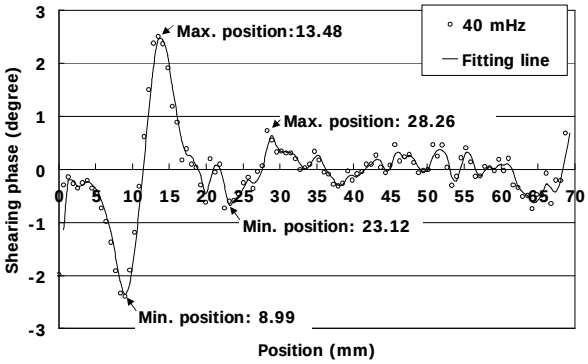

(b) Shearing phase

Figure 9: *Quantitative determination of the size and the location of defects on specimen III*

The maximum and minimum points of 1 *mm* deep defect are distinguishable and the size is estimated as 4.5 *mm* and the location is at 12 *mm*. The defect at 3 *mm* depth referred to Fig. 10(a) is as 5.14 *mm* and is at 17.5 *mm* respectively. It is more difficult to detect a slender void defect close to each other due to small phase difference and low pixel resolution and it is difficult to apply shearing phase technique for the contrast of phase difference, less than 4 degree.

5. Conclusions

The paper proposes the quantitative determination the size and location of subsurface defects by shearing phase technique, in which the slope of phase contrast at optimum thermal wave frequency is extracted by the subtraction between adjacent pixels. The shearing phase distribution has maximum, minimum, and zero point, which is a key to estimate the size and location of defects. Steel plate specimens with defects at different shape, size, and depth are inspected and the results shows good agreement compared with actual values. Although defect sizing is achieved by high-performance image processing technique or neural network interpreter, the proposed technique can easily estimate the size and location of a defect with high accuracy. Since a clear edge boundary condition of these defects induces apparent phase slope points which are somewhat different condition in practical well thinning or inside void defects, advanced studies for a spherical boundary is required.

6. References

[1] Maldague, X. P. V., *Theory and Practice of Infrared Technology for Nondestructive Testing*, John Wiley & Sons, New York, 2001.

[2] Maldague, X. P. V., *Trends in optical nondestructive testing and inspection*, Rastogi P.K., Inaudi D, editors, Elsevier Science, Switzerland, 2000.

[3] Busse, G.., Wu, D., and Karpen, W., "Thermal wave imaging with phase sensitive modulated thermography," *J. Appl. Phys.*, 71(8):3962-3965, 1992.

[4] Wu, D., and Busse, G.., "Lock-in thermography for nondestructive evaluation of materials," *Rev. Gen. Therm.*, 37:693-703, 1998.

[5] Wu, D., Salerno, A., Schonbach, B., Hallin, H., and Busse, C., "Phase-sensitive modulation thermography and its applications for NDE," *Proc. of SPIE*, 3056:176-182, 1997.

[6] Achenbach, J.D., Rajapakse, Y. ed., *Solid Mechanics Research for Quantitative Non-Destructive Evaluation (QNDE)*, Springer, London, 1988.

[7] Almond, D. P. and Lau, S. K., "Defect sizing by transient thermography. I: an analytical treatment", *J. Phys. D: Appl. Phys.*, 27:1063-1069, 1994.

[8] Saintey, M. B. and Almond, D. P., "An artificial neural network interpreter for transient thermography image data", *NDT&E International*, 30(5):291-295, 1997.

[9] Ibarra-Castanedo, C., González, D., Klein, M., Pilla, M. Vallerand, S. Maldague, X., "Infrared image processing and data analysis", *Infrared Physics & Technology*, 46:75–83, 2004.

[10] Carlomagno, G. M., Berardi, P. G., "Unsteady thermotopography in non-destructive testing". In: Warren C., editor. *Proceedings of the III infrared information exchange*, 33–40, 1976.

[11] Bai, W. and Wong, B. S., "Evaluation of Defects in Composite Plates under Convective Environments using Lock-In Thermography," *Meas. Sci. Technol*. 12:142-150, 2001.